Chemical Science

ROYAL SOCIETY OF CHEMISTRY

EDGE ARTICLE

View Article Online
View Journal | View Issue

Cite this: *Chem. Sci.*, 2020, **11**, 2381

All publication charges for this article have been paid for by the Royal Society of Chemistry

Intra- and intermolecular interception of a photochemically generated terminal uranium nitride†

Munendra Yadav, * Alejandro Metta-Magaña and Skye Fortier *

Received 26th November 2019
Accepted 21st January 2020

DOI: 10.1039/c9sc05992j

rsc.li/chemical-science

The photochemically generated synthesis of a terminal uranium nitride species is here reported and an examination of its intra- and intermolecular chemistry is presented. Treatment of the U(III) complex $L^{Ar}UI(DME)$ ($(L^{Ar})^{2-}$ = 2,2″-bis(Dippanilide)-*p*-terphenyl; Dipp = 2,6-diisopropylphenyl) with $LiNIm^{Dipp}$ ($(NIm^{Dipp})^{-}$ = 1,3-bis(Dipp)-imidazolin-2-iminato) generates the sterically congested 3N-coordinate compound $L^{Ar}U(NIm^{Dipp})$ (**1**). Complex **1** reacts with 1 equiv. of Ph_3CN_3 to give the U(IV) azide $L^{Ar}U(N_3)(NIm^{Dipp})$ (**2**). Structural analysis of **2** reveals inequivalent N_α–N_β > N_β–N_γ distances indicative of an activated azide moiety predisposed to N_2 loss. Room-temperature photolysis of benzene solutions of **2** affords the U(IV) amide (*N*-L^{Ar})$U(NIm^{Dipp})$ (**3**) *via* intramolecular N-atom insertion into the benzylic C–H bond of a pendant isopropyl group of the $(L^{Ar})^{2-}$ ligand. The formation of **3** occurs as a result of the intramolecular interception of the intermediately generated, terminal uranium nitride (L^{Ar})U(N)(NIm^{Dipp}) (**3′**). Evidence for the formation of **3′** is further bolstered by its intermolecular capture, accomplished by photolyzing solutions of **2** in the presence of an isocyanide or PMe_3 to give (L^{Ar})U[NCN($C_6H_3Me_2$)](NIm^{Dipp}) (**5**) and (*N*,*C*-L^{Ar}*)U(N=PMe_3)(NIm^{Dipp}) (**6**), respectively. These results expand upon the limited reactivity studies of terminal uranium–nitride moieties and provide new insights into their chemical properties.

Introduction

The study of metal–ligand multiple bonds has played a critical role in the understanding and development of d-block reactivity profiles[1] and continues to be a widely studied area of interest. In comparison, the chemistry of actinide–ligand multiple bonding has lagged substantially behind. This is due in part to the poor radial extension of the actinide 5f valence orbitals, potential energetic mismatch between the metal and ligand bonding orbitals, and a higher degree of ionic bonding character,[2] which can favour bridging and formation of higher nuclearity complexes. Despite these challenging factors, significant advances in early actinide–ligand multiple bonding have been achieved in recent years,[3] from the synthesis of imido and heavier chalcogenide analogues of the pervasive uranyl cation, UO_2^{2+} (*e.g.*, $U(N^tBu)_2I_2(THF)_2$);[4] $[Cp^*_2Co][U(E)(O)(NR_2)_3]$ (R = $SiMe_3$; E = S, Se),[5] to the synthesis of uranium tris- and tetrakis(imido) complexes and beyond.[6]

Notably, special efforts have been dedicated over the years to the synthesis and isolation of uranium compounds possessing terminal nitride moieties. In contrast to the well-developed nitride chemistry of the transition metals,[7] complexes featuring U≡N bonds were once considered a so-called "holy grail" of actinide chemistry as results were long limited to matrix isolation experiments and systems containing bridging nitride moieties.[8] The paucity of these compounds is surprising as the uranium–oxygen bonds of uranyl (UO_2^{2+}) are remarkably robust and share an isolobal U≡O bonding relationship to U≡N functionalities. Moreover, complexes featuring terminal uranium-oxo bonds, once rare, are now fairly well-known.[3,5,9]

It bears mentioning that the study of bridged actinide nitrides of the type An=N=An has proven a to be a fruitful area of investigation with rich chemistry.[6e,10] This has included such novel transformations as the cleavage of CO by [Cs{[U(OSi(O^{t}Bu)$_3$)$_3$]$_2$(μ-N)}] to give the bridged cyanide complex [Cs{[U(OSi(O^{t}Bu)$_3$)$_3$]$_2$(μ-CN)(μ-O)}][10c] as well as reversible dihydrogen activation by the same bridged nitride complex to give the hydride imide [Cs{U(OSi(O^{t}Bu)$_3$)$_3$}$_2$(μ-H)(μ-NH)].[10g]

In 2010, a major milestone was reached when Kiplinger and co-workers provided evidence for the intermediate formation of a terminal uranium–nitride species generated through the photolysis of the U(IV) azide $Cp^*_2U[N(SiMe_3)_2](N_3)$ to give the intramolecularly C–H activated product $Cp^*(\eta^5\text{-}C_5Me_4CH_2NH)U[N(SiMe_3)_2]$.[11] This result demonstrated that terminal uranium

Department of Chemistry and Biochemistry, University of Texas at El Paso, El Paso, TX 79968, USA. E-mail: asfortier@utep.edu

† Electronic supplementary information (ESI) available: Experimental details and procedures, additional crystallographic information, and NMR spectral data. CCDC 1958453, 1958456, 1958640, 1958626 and 1958455. For ESI and crystallographic data in CIF or other electronic format see DOI: 10.1039/c9sc05992j

nitrides are photochemically accessible but suggested an inherent instability. A few years later, in a landmark result, Liddle and co-workers established that not only could terminal uranium nitrides be synthesized but could also be isolated when using an appropriate ligand architecture under specific reaction conditions. Namely, they showed that treatment of the bulky U(III) complex U(Tren^{TIPS}) (Tren^{TIPS} = [N(CH$_2$CH$_2$NSi^{i}Pr$_3$)$_3$]$^{3-}$) with NaN$_3$ gives the mononuclear U(V) nitride [Na(12-crown-4)$_2$][U(≡N)(Tren^{TIPS})] upon workup and addition of 12-crown-4 polyether, though this compound is sensitive and rapidly decomposes in ethereal solutions.[12] A follow-up study showed that oxidation with molecular iodine affords access to the hexavalent, terminal nitride U(≡N)(Tren^{TIPS}).[13] On the heels of this, Cloke *et al.*, using a bulky U(III) metallocene platform treated with NaN$_3$, reported the synthesis and structural characterization of the sodium-capped U(V) nitride [C$_8$H$_6$(Si^{i}Pr$_3$)$_2$]Cp*U(≡N)Na(OEt$_2$)$_2$.[14]

Critically, these nitride complexes provide valuable new insights into the area of actinide metal–ligand multiple bonding; however, given the rarity of these species, much remains to be learned regarding the reactivity of U≡N bonds with studies thus far largely limited to Liddle's system. For instance, [Na(12-crown-4)$_2$][U(N)(Tren^{TIPS})] reacts with Me$_3$SiCl to give the imide U(NSiMe$_3$)(Tren^{TIPS}),[12] while [U(N)(Tren^{TIPS})]$^{n-}$ (n = 0, 1) is reactive towards CE$_2$ (E = O, S) heteroallenes leading to the formation of U(O)(Tren^{TIPS}) and U-NCE products through multiple bond metathesis and complex redox pathways.[9l] On this note, [U(N)(Tren^{TIPS})]$^{n-}$ (n = 0, 1) is susceptible to reductive carbonylation upon addition of CO, leading to the formation of U-NCO isocyanates.[15]

Furthermore, evidence is beginning to mount which shows the reactivity of mononuclear uranium nitrides to be particularly distinct from other uranium–ligand multiple bonds as they appear to show a propensity for C–H bond activation chemistry. As in the case of the putative Cp*$_2$U(N)[N(SiMe$_3$)$_2$],[11] photolysis of U(N)(Tren^{TIPS}) gives rise to the U(IV) N-atom inserted amide U[N(CH$_2$CH$_2$NSi^{i}Pr$_3$)$_2$(CH$_2$CH$_2$NSi^{i}Pr$_2$CHMeCH$_2$N)].[13] More recently, it was shown that the one-electron reduction of the U(IV) bisazide (PN)$_2$U(N$_3$)$_2$ (PN = N(2-^{i}Pr$_2$P-4-MeC$_6$H$_3$)(2,4,6-Me$_3$C$_6$H$_2$)) does not lead to the formation of a U(V) nitride but instead generates the potassium-capped parent imido complex [K(THF)$_3$]{(PN)U(NH)[^{i}Pr$_2$P(C$_6$H$_3$Me)N(C$_6$H$_2$Me$_2$CH$_2$)]} by way of intramolecular C–H bond addition of a pendant methyl group.[16]

In our laboratory, we have been exploring the chemistry of uranium supported by a bis(anilide) terphenyl ligand ((L^{Ar})$^{2-}$). In the complex L^{Ar}UI(DME) (**A**) (Scheme 1), the uranium is straddled between two nitrogen atoms in a nearly linear fashion with the metal situated above the central ring of the terphenyl moiety with steric protection afforded by encumbering 2,6-diisopropylphenyl (Dipp) groups.[17] This platform has been shown able to support a rare U–Fe actinide–metal bond,[17] and we reasoned that the [L^{Ar}U] system may be suitable for accessing other unique bonding motifs with uranium, such as U≡N bonds. Here, we present our synthesis of a uranium nitride complex and present its intra- and intermolecular reactivity, thus expanding the limited portfolio of terminal actinide–nitride chemistry.

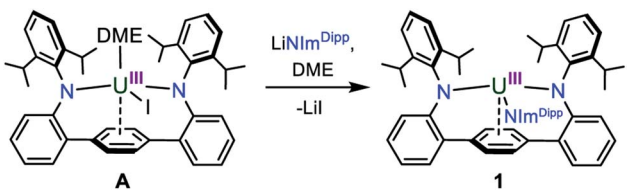

Scheme 1 Synthesis of **1**.

Results and discussion

In an effort to enhance the relative electron richness of our [L^{Ar}U] platform, while adding increased steric protection to disfavour possible U–N–U cluster formation, the 1,3-bis(Dipp) imidazolin-2-iminato (Im^{Dipp}N$^-$) ligand was reacted with **A** to give the 3N-coordinated U(III) complex L^{Ar}U(NIm^{Dipp}) (**1**) (Scheme 1). Complex **1** is isolated in 36% yield as dark brown crystals from the storage of concentrated DME solutions at −22 °C for 2 days.

The solid-state molecular structure of **1**·DME reveals a highly congested uranium centre, which is effectively illustrated through its space-filling model (Fig. 1). As compared to the uranium–anilide distances of **A** (U–N = 2.524(4)–2.558(3) Å), the U1–N1 = 2.429(3) Å and U1–N2 = 2.369(3) Å bonds are significantly shorter, while the N1–U1–N2 = 128.8(1)° bond

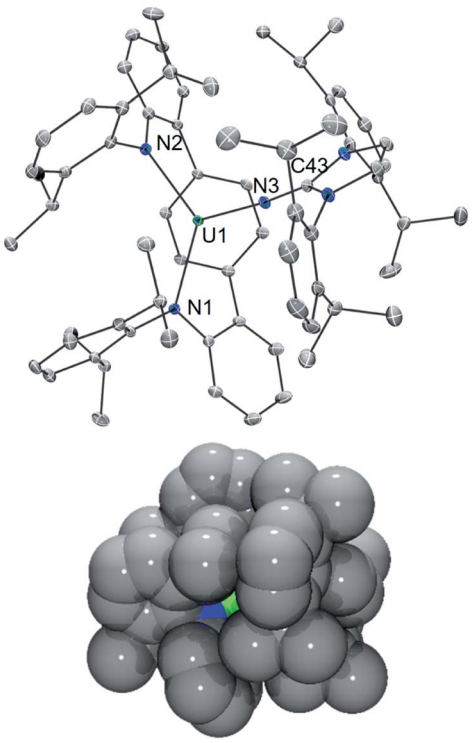

Fig. 1 Solid-state molecular structure of **1**·DME (top). Space filling model of **1** showing uranium (green), nitrogen (blue), and carbon (gray) atom spheres (bottom).

angle is now nearly thirty degrees more acute. Of note, the distance between the uranium and the central ring of the terphenyl ligand (U–$C_{centroid}$ = 2.38 Å) in **1**·DME also contracts substantially as compared to **A** (U–$C_{centroid}$ = 2.56 Å). We ascribe the significant structural changes within the [L^{Ar}U] core from **A** to **1**·DME as a consequence of having to accommodate the sterically imposing $Im^{Dipp}N^{-}$ ligand.

It should be noted that the coordination of iminic N-donor ligands to U(III) is rare, and inspection of the U–NIm bond length in **1**·DME (U1–N3 = 2.169(3) Å) reveals it to be much shorter than the non-bridging uranium–ketimide bond in the inverted sandwich complex [$Na_2(Et_2O)$][UN(^{t}Bu)(Mes)]$_2$(μ:η^6-C_7H_8) (U–N = 2.24(1) Å).[18] However, the U–NIm bonding metrics (U1–N3 = 2.169(3) Å; U1–N3–C43 = 170.4(3)°) are similar to that reported for tetravalent U(NIm^{Dipp})[$N(SiMe_3)_2$]$_3$ (U–N = 2.137(6) Å; U–N–C = 169.5(5)°).[19]

With **1** in hand, addition of 1 equiv. of Me_3SiN_3 in DME at room temperature leads to the formation of the U(IV) complex $L^{Ar}U(N_3)(NIm^{Dipp})$ (**2**). Compound **2** is produced in low yield and is accompanied by the formation of $(Me_3Si)_2L^{Ar}$. As the reaction appears to proceed *via* the one-electron reduction of Me_3SiN_3, we reasoned that Ph_3CN_3 would be a viable azide source as reduction would lead to the formation of Gomberg's dimer which should avoid back-reactions with the ligand. As such, use of Ph_3CN_3 with U[$N(SiMe_3)_2$]$_3$ generates the U(IV) azide U(N_3)[$N(SiMe_3)_2$]$_3$.[9i] Accordingly, treatment of **1** with Ph_3CN_3 in C_6D_6 at room temperature leads to the quantitative formation of **2** as observed by ^{1}H NMR spectroscopy. The reaction can be performed on a preparative scale at room temperature in solutions of toluene with crystals of **2** generated from the diffusion of hexanes into concentrated toluene/benzene solutions stored at −22 °C, providing **2** in 57% isolated yield (Scheme 2).

The solid-state molecular structure of **2**·C_6H_6 is shown in Fig. 2. Interestingly, oxidation to U(IV) leads to an elongation of the U–L^{Ar} bonds (U1–N1 = 2.455(5) Å; U1–N2 = 2.414(5) Å; U–$C_{centroid}$ = 2.58 Å). On the other hand, the U–NIm bond is observed to undergo contraction (U1–N3 = 2.135(4) Å). Of particular note, the U–N_3 distance (U1–N6 = 2.142(5) Å) is on the shorter end of the range reported for tetravalent uranium azides (2.22–2.56 Å).[20] Moreover, the azide unit exhibits

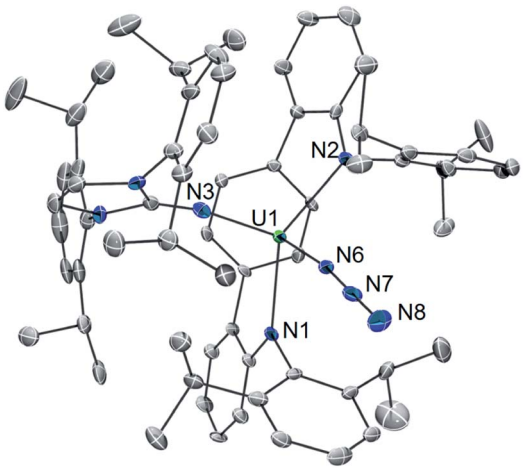

Fig. 2 Solid-state molecular structure of **2**·C_6H_6.

inequivalent nitrogen–nitrogen distances (N6–N7 = 1.24(1) Å, N7–N8 = 1.13(2) Å) which indicates activation of the azide moiety. Together, the short U–N_3 bond and azide activation is characteristic of what has been described in the literature as a covalent metal–azide interaction.[21]

Complex **2** is soluble in ethereal solvents while possessing moderate solubility in aromatic solvents such as benzene and toluene. The ^{1}H NMR spectrum of **2** in toleuene-d_8 is complicated, giving rise to 50 distinct resonances appearing from −22.3 to 28.9 ppm (see ESI Fig. SI3 and SI4†), which we attribute to increased rotational restriction owing to occupation of the axial position by the azide unit. Accordingly, each of the 16 methyl groups of the isopropyl functionalities in **2** gives rise to a unique resonance integrating to three protons each.

Attempts to reduce **2** with external reductants such as KC_8 or [Li(18-crown-6)][biphenyl][22] inevitably led to the formation of alkali metal salts of the $(L^{Ar})^{2-}$ ligand. Additionally, treatment of **2** with strong Lewis acids (*e.g.* Sm(OTf)$_3$) also failed to initiate N_2 loss. Furthermore, thermolysis of C_6D_6 solutions of **2** up to refluxing temperatures does not lead to any change within the ^{1}H NMR spectrum.

Gratifyingly, photolyzing solutions of **2** with UV light (365 nm) for at least 24 hours does lead to new reactivity. This generates a paramagnetic species with a ^{1}H NMR spectrum that features 50 resonances within the range of −56.6 to 97.0 ppm (see ESI Fig. SI6†). Removal of the solvent and recrystallisation from hexanes provides crystals of the C_1 symmetric U(IV) N-atom inserted product (*N*-L^{Ar})U(NIm^{Dipp}) (**3**·C_6H_{14}) (Scheme 2), and its solid-state molecular structure is depicted in Fig. 3.

Overall, the structural changes as compared to **2**·C_6H_6 are modest (**3**·C_6H_{14}: U1–N1 = 2.415(3) Å, U1–N2 = 2.388(3) Å, U1–N3 = 2.159(3) Å); yet, the uranium atom does become offset from the central terphenyl ring moving from a nominal η^6 interaction to a η^4 orientation. By far, the most salient feature of **3**·C_6H_{14} is the formation of a new U–amide bond (U1–N6 = 2.167(3) Å) from insertion of a nitrogen atom into a pendant isopropyl group of the $(L^{Ar})^{2-}$ ligand. This result is strongly reminiscent of the chemistry observed in the photolysis of

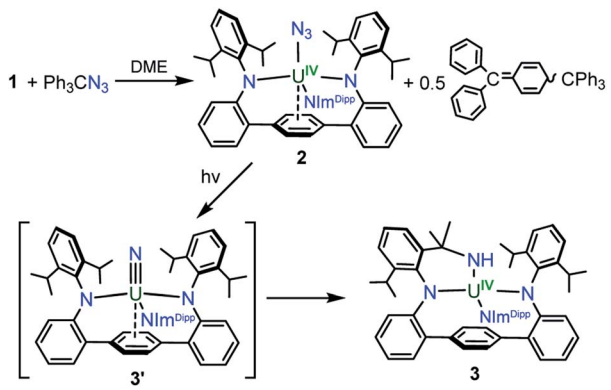

Scheme 2 Synthesis of **2** and proposed formation of **3** *via* terminal nitride **3′**.

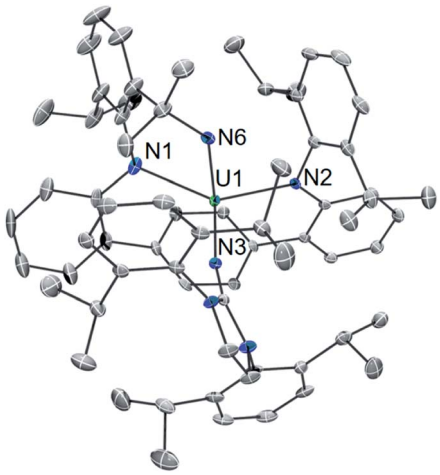

Fig. 3 Solid-state molecular structure of $3\cdot C_6H_{14}$.

$Cp^*_2U[N(SiMe_3)_2](N_3)$ and $U(N)(Tren^{TIPS})$,[11,13] providing strong evidence for the passing formation of $(L^{Ar})U(N)(NIm^{Dipp})$ (**3′**) possessing a terminal uranium nitride bond (Scheme 2). And, as with these systems, the ligand in **2** acts to intercept the nitride through intramolecular trapping.

The formation of **3′** begs the question of the formal oxidation state assignment of its uranium centre. The elimination of N_2 from the azide unit is typically a two-electron process, which would render a U(VI) assignment for a diamagnetic **3′**. Yet, formation of radical or nitrene character at the nitride moiety clouds canonical oxidation state assignments. Following the photoreaction by ^{1}H NMR and UV-vis spectroscopies (see ESI Fig. SI5 and SI13†) shows the conversion of **2** to **3** without the apparent formation of any intermediate species. Furthermore, following the low temperature photolysis of **2** in toluene-d_8 at −10 °C by ^{1}H NMR spectroscopy also fails to trap or detect a fleeting species. This suggests that the nitride intermediate formed in the reaction is highly reactive and undergoes rapid reactivity with the ligand.

In an effort to chemically intercept **3′**, CO was added to a C_6D_6 solution of **2**. Upon addition, the immediate appearance of a complex series of resonances is observed in the ^{1}H NMR spectrum concomitant with partial consumption of the starting material. The reaction is complete in 12 hours at room temperature. Workup of the reaction mixture and crystallisation from a hexanes/Et_2O solution provides small yellow crystals of the U(IV) compound $(CO\text{-}L^{Ar})U(N_3)(NIm^{Dipp})$ (**4**) in low yield, formed from insertion of CO into a uranium–anilide bond (Scheme 3). Photolysis of **2** in the presence of a CO atmosphere also leads to the formation of **4** as the only isolable product. While such reactivity is not well-documented among 5f-element amide compounds, it has been previously reported in the reactions of $Cp^*_2M(NR_2)_2$ (M = Th, U, R = CH_3; M = U, R = C_2H_5) with CO to give $Cp^*_2M(\eta^2\text{-}CO\text{-}NR_2)_2$.[23]

Weak X-ray diffraction data for **4** precludes an in-depth structural analysis, but connectivity is definitively established (see ESI Fig. SI1†) and shows the carbonyl moiety binds to the uranium in an η^2-fashion. Photolysis of solutions of **4** does not result in any observed reactivity, signalling that the U–N_3 interaction is highly sensitive to the coordination environment of the uranium metal centre.

Using a bulky isocyanide to prevent ligand insertion, room temperature photolysis of **2** in the presence of $C{\equiv}N(C_6H_3Me_2)$ in C_6D_6 results in the formation of a new paramagnetic species as indicated by ^{1}H NMR spectroscopy (see ESI Fig. SI8†). Removal of the solvent and extraction into a mixture of diethyl ether and hexanes followed by storage at −22 °C for 4 days affords dark brown-red crystals in 44% yield. Analysis by single crystal X-ray diffraction revealed the formation of the U(IV) carbodiiminate complex $(L^{Ar})U[NCN(C_6H_3Me_2)](NIm^{Dipp})$ ($\mathbf{5}\cdot Et_2O$) (Scheme 4) and (Fig. 4).

The core $[(L^{Ar})U(NIm^{Dipp})]^+$ structure of $\mathbf{5}\cdot Et_2O$ (U1–N1 = 2.408(3) Å, U1–N2 = 2.450(3) Å, U1–N3 = 2.136(3) Å, U1–$C_{centroid}$ = 2.58 Å, N1–U1–N2 = 142.6(1)°) is similar to that found for $\mathbf{2}\cdot C_6H_6$. Moreover, the uranium–carbodiiminate bond (U1–N6 = 2.235(3) Å) is longer in length than the U–N_3 bond in $\mathbf{2}\cdot C_6H_6$ but much shorter than the U–N_{carbo} bond found in the U(IV) triazacyclononane tris(aryloxide) complex $[(^tBuArO)_3tacn]U(NCNMe)$ (U–N = 2.327(3) Å), formed by a multiple-bond metathesis reaction that proceeds *via* nitrene transfer between $[(^tBuArO)_3tacn]U{=}NSiMe_3$ and CNMe.[24]

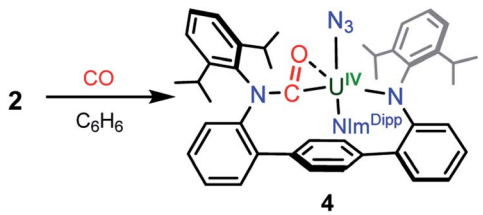

Scheme 3 Synthesis of **4**.

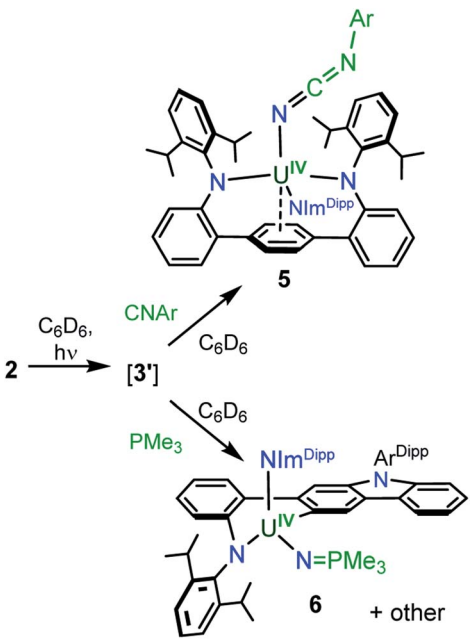

Scheme 4 Synthesis of **5** and **6**.

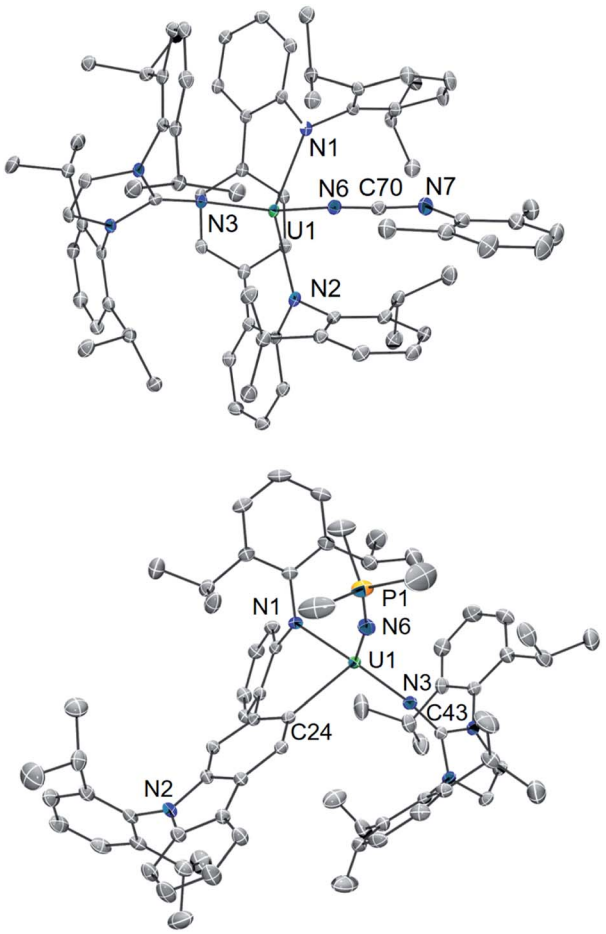

Fig. 4 Solid-state molecular structures of $5{\cdot}Et_2O$ (top) and $6{\cdot}Et_2O$ (bottom).

Furthermore, photolyzing benzene solutions of **2** with a slight excess of PMe_3 leads to a highly complicated mixture of products as shown through ^1H NMR spectroscopy. From these mixtures, one major product is reproducibly isolated in approximately 15% yield as yellow crystals, though separation of pure material has been hampered by co-crystallisation of other as-of-yet unidentified products. The ^1H NMR spectrum of the major product in C_6D_6 is suggestive of C_1 symmetry in solution as it exhibits 51 distinct resonances with 19 peaks attributable to the three protons of each methyl group (see ESI Fig. SI10†). Moreover, only one resonance in the $^{31}P\{^1H\}$ NMR spectrum is observed in the reaction mixture, appearing at 12.1 ppm (see ESI Fig. SI11†).

In line with this, the solid-state molecular structure of the yellow crystals obtained through X-ray diffraction analysis revealed the formation of the asymmetric, arylated U(IV) phosphinimide (N,C-L^{Ar}*)U(N=PMe_3)(NIm^{Dipp}) (**6**) (Scheme 4). As seen in Fig. 4, a number of structural and chemical changes occur including ligand cyclization to give a carbazole functionality accompanied by deprotonation of the central terphenyl ring to give a U–C_{aryl} bond (U1–C24). Nonetheless, clearly present in $6{\cdot}Et_2O$ is the formation of a –N=PMe_3 group (U1–N6 = 2.115(2) Å; U1–N6–P1 = 161.7(2)°), with metrical parameters comparable to its U–NIm interaction (U1–N3 = 2.141(2) Å; U–N3–C43 = 168.8(2)°) and the U–N=PPh_3 bond in Cp_3UNPPh_3 (U–N = 2.07(2) Å; U–N–P = 172(1)°).[25] We reason that upon formation of the phosphinimide, steric congestion forces structural rearrangement, consequently initiating a cascade of chemical events that gives the complicated product mixture containing **6**. Photolysis in the presence of the more encumbered phosphine, PMe_2Ph, leads exclusively to the formation of **3**.

Importantly, complex **2** does not react with C≡N($C_6H_3Me_2$) or PMe_3 in the absence of light, and the formation of **5** and **6** occur exclusively under photolysis. This proves that **3′** is a key intermediate and a sufficiently long-lived species such that it is susceptible to chemical trapping, bypassing competitive intramolecular C–H insertion pathways. Moreover, the formation of these complexes represents the first examples of intermolecular chemistry for a photochemically generated uranium nitride.

The reactivity of **3′** with nucleophiles is akin to that observed for the reductive carbonylation of $U^{VI}(N)(Tren^{TIPS})$ with CO to give $U^{IV}(NCO)(Tren^{TIPS})$,[15] and while **3′** is a putative terminal nitride, its reactivity is further reminiscent of the chemistry between dinuclear $\{[U(N^tBuAr)_3]_2(\mu\text{-}N)\}^+$ (Ar = 3,5-dimethylphenyl) and CN^- which generates the bridged carbodiiminate $[U(N^tBuAr)_3]_2(\mu\text{-}NCN)$.[26] Overall, the formation of **3**, **5**, and **6** through partial N-atom transfer concomitant with reduction of the metal centre is, from first principles, consistent with classic electrophilic nitride character. While we favour this particular perspective, we acknowledge it may be an oversimplification as uranium nitrides have been demonstrated to exhibit ambiphilic character. For instance, DFT analysis indicates that the reaction of $U(N)(Tren^{TIPS})$ with CO proceeds through donation of the nitride lone-pair into the CO π*-orbital, signalling initiation *via* nucleophilic attack of the nitride onto CO.[14] This is not unlike the reactivity profile known for some terminal iron nitrides which have also been described as possessing a dual-nature transition state, where the nitride simultaneously exhibits both nucleophilic and electrophilic character in the reactions of $PhB(MesIm)_3Fe{\equiv}N$ ($PhB(MesIm)_3$ = tris(mesitylcarbene) borate)[27] and $[L^{Ar*}]FeN(py)$ (L^{Ar*} = ($^tBu_2CN$)C(Ar*N)$_2$, Ar* = 2,6-bis(diphenylmethyl)-4-*tert*-butylphenyl)[28] with phosphines to give [Fe–N=PMe_3] products. As such, this reveals an interesting reactivity pattern for uranium nitrides, and further study of **3′** is underway to better elucidate the reactivity character of its nitride group.

Conclusion

In closing, while the landmark isolation of monouranium nitrides have been achieved through the synthesis of $[U(N)(Tren^{TIPS})]^{n-}$ (n = 0, 1) and $[C_8H_6(Si^iPr_3)_2]Cp^*U({\equiv}N)Na(OEt_2)_2$ by the groups of Liddle and Cloke, respectively,[12–14] much remains to be learned regarding the character of UN bonds. Here, we have demonstrated that $L^{Ar}U(N_3)(NIm^{Dipp})$ (**2**) provides an accessible platform for testing such reactivity as its photolysis generates the $(L^{Ar})U(N)(NIm^{Dipp})$ (**3′**) intermediate which can be intra- and intermolecularly intercepted. In the latter case, addition of the nucleophiles C≡N($C_6H_3Me_2$) and

PMe_3 to **3′** gives the U(IV)–imine products (L^{Ar})U[NCN(C_6H_3-Me_2)](NIm^{Dipp}) (**5**) and (*N*,*C*-L^{Ar}*)U(N=PMe_3)(NIm^{Dipp}) (**6**), respectively, produced as a result of nitride capture and partial N-atom transfer. Thus, for the first time, we demonstrate that accessing intermolecular uranium–nitride chemistry under photochemical conditions is possible. These reactions can be classically described as proceeding through an electrophilic nitride, though the potential for nitride ambiphilicity cannot be ruled out at this stage and a thorough reaction survey of **3′** with other substrates is ongoing.

Conflicts of interest

There are no conflicts to declare.

Acknowledgements

We are grateful to the Welch Foundation (AH-1922-20170325) and the NSF PREM Program (DMR-1827745) for financial support of this work. S. F. is an Alfred P. Sloan Foundation research fellow and is thankful for their support. We also wish to acknowledge the NSF-MRI program (CHE-1827875) for providing funding for the purchase of an X-ray diffractometer.

Notes and references

1 W. A. Nugent and J. M. Mayer, *Metal-Ligand Multiple Bonds*, John Wiley & Sons, New York, 1988.

2 (*a*) S. T. Liddle, *Angew. Chem., Int. Ed.*, 2015, **54**, 8604–8641; (*b*) M. L. Neidig, D. L. Clark and R. L. Martin, *Coord. Chem. Rev.*, 2013, **257**, 394–406; (*c*) R. Beekmeyer and A. Kerridge, *Inorganics*, 2015, **3**, 482–499; (*d*) W. W. Lukens, M. Speldrich, P. Yang, T. J. Duignan, J. Autschbach and P. Kogerler, *Dalton Trans.*, 2016, **45**, 11508–11521.

3 (*a*) T. W. Hayton, *Chem. Commun.*, 2013, **49**, 2956–2973; (*b*) T. W. Hayton, *Dalton Trans.*, 2010, **39**, 1145–1158.

4 T. W. Hayton, J. M. Boncella, B. L. Scott, P. D. Palmer, E. R. Batista and P. J. Hay, *Science*, 2005, **310**, 1941–1943.

5 J. L. Brown, S. Fortier, G. Wu, N. Kaltsoyannis and T. W. Hayton, *J. Am. Chem. Soc.*, 2013, **135**, 5352–5355.

6 (*a*) N. H. Anderson, S. O. Odoh, Y. Y. Yao, U. J. Williams, B. A. Schaefer, J. J. Kiernicki, A. J. Lewis, M. D. Goshert, P. E. Fanwick, E. J. Schelter, J. R. Walensky, L. Gagliardi and S. C. Bart, *Nat. Chem.*, 2014, **6**, 919–926; (*b*) N. H. Anderson, J. Xie, D. Ray, M. Zeller, L. Gagliardi and S. C. Bart, *Nat. Chem.*, 2017, **9**, 850–855; (*c*) B. M. Gardner, G. Balazs, M. Scheer, F. Tuna, E. J. L. McInnes, J. McMaster, W. Lewis, A. J. Blake and S. T. Liddle, *Nat. Chem.*, 2015, **7**, 582–590; (*d*) E. P. Wildman, G. Balazs, A. J. Wooles, M. Scheer and S. T. Liddle, *Nat. Commun.*, 2017, **8**, 14769; (*e*) S. L. Staun, D. C. Sergentu, G. Wu, J. Autschbach and T. W. Hayton, *Chem. Sci.*, 2019, **10**, 6431–6436; (*f*) W. S. Ren, G. F. Zi, D. C. Fang and M. D. Walter, *J. Am. Chem. Soc.*, 2011, **133**, 13183–13196; (*g*) N. L. Bell, L. Maron and P. L. Arnold, *J. Am. Chem. Soc.*, 2015, **137**, 10492–10495; (*h*) C. C. Zhang, G. H. Hou, G. F. Zi and M. D. Walter, *Dalton Trans.*, 2019, **48**, 2377–2387.

7 (*a*) J. M. Smith, *Prog. Inorg. Chem.*, 2014, **58**, 417–470; (*b*) J. F. Berry, *Comments Inorg. Chem.*, 2009, **30**, 28–66; (*c*) K. Dehnicke and J. Strahle, *Angew. Chem., Int. Ed.*, 1992, **31**, 955–978.

8 D. M. King and S. T. Liddle, *Coord. Chem. Rev.*, 2014, **266–267**, 2–15.

9 (*a*) A. J. Lewis, P. J. Carroll and E. J. Schelter, *J. Am. Chem. Soc.*, 2013, **135**, 13185–13192; (*b*) A. J. Lewis, P. J. Carroll and E. J. Schelter, *J. Am. Chem. Soc.*, 2013, **135**, 511–518; (*c*) C. J. Hoerger, H. S. La Pierre, L. Maron, A. Scheurer, F. W. Heinemann and K. Meyer, *Chem. Commun.*, 2016, **52**, 10854–10857; (*d*) N. S. Settineri, A. A. Shiau and J. Arnold, *Chem. Commun.*, 2018, **54**, 10913–10916; (*e*) S. M. Franke, B. L. Tran, F. W. Heinemann, W. Hieringer, D. J. Mindiola and K. Meyer, *Inorg. Chem.*, 2013, **52**, 10552–10558; (*f*) O. Cooper, C. Camp, J. Pecaut, C. E. Kefalidis, L. Maron, S. Gambarelli and M. Mazzanti, *J. Am. Chem. Soc.*, 2014, **136**, 6716–6723; (*g*) A. C. Schmidt, F. W. Heinemann, W. W. Lukens and K. Meyer, *J. Am. Chem. Soc.*, 2014, **136**, 11980–11993; (*h*) D. M. King, F. Tuna, J. McMaster, W. Lewis, A. J. Blake, E. J. L. McInnes and S. T. Liddle, *Angew. Chem., Int. Ed.*, 2013, **52**, 4921–4924; (*i*) K. C. Mullane, A. J. Lewis, H. Yin, P. J. Carroll and E. J. Schelter, *Inorg. Chem.*, 2014, **53**, 9129–9139; (*j*) D. P. Halter, F. W. Heinemann, J. Bachmann and K. Meyer, *Nature*, 2016, **530**, 317; (*k*) K. C. Mullane, T. Cheisson, E. Nakamaru-Ogiso, B. C. Manor, P. J. Carroll and E. J. Schelter, *Chem.–Eur. J.*, 2018, **24**, 826–837; (*l*) P. A. Cleaves, C. E. Kefalidis, B. M. Gardner, F. Tuna, E. J. L. McInnes, W. Lewis, L. Maron and S. T. Liddle, *Chem.–Eur. J.*, 2017, **23**, 2950–2959; (*m*) S. J. Kraft, J. Walensky, P. E. Fanwick, M. B. Hall and S. C. Bart, *Inorg. Chem.*, 2010, **49**, 7620–7622.

10 (*a*) L. Chatelain, R. Scopelliti and M. Mazzanti, *J. Am. Chem. Soc.*, 2016, **138**, 1784–1787; (*b*) M. Falcone, L. Chatelain and M. Mazzanti, *Angew. Chem., Int. Ed.*, 2016, **55**, 4074–4078; (*c*) M. Falcone, C. E. Kefalidis, R. Scopelliti, L. Maron and M. Mazzanti, *Angew. Chem., Int. Ed.*, 2016, **55**, 12290–12294; (*d*) M. Falcone, L. Chatelain, R. Scopelliti and M. Mazzanti, *Chimia*, 2017, **71**, 209–212; (*e*) M. Falcone, L. Chatelain, R. Scopelliti, I. Zivkovic and M. Mazzanti, *Nature*, 2017, **547**, 332–335; (*f*) M. Falcone and M. Mazzanti, *Chimia*, 2018, **72**, 199–202; (*g*) M. Falcone, L. N. Poon, F. F. Tirani and M. Mazzanti, *Angew. Chem., Int. Ed.*, 2018, **57**, 3697–3700; (*h*) L. Barluzzi, L. Chatelain, F. Fadaei-Tirani, I. Zivkovic and M. Mazzanti, *Chem. Sci.*, 2019, **10**, 3543–3555; (*i*) M. Falcone, L. Barluzzi, J. Andrez, F. F. Tirani, I. Zivkovic, A. Fabrizio, C. Corminboeuf, K. Severin and M. Mazzanti, *Nat. Chem.*, 2019, **11**, 154–160; (*j*) C. T. Palumbo, L. Barluzzi, R. Scopelliti, I. Zivkovic, A. Fabrizio, C. Corminboeuf and M. Mazzanti, *Chem. Sci.*, 2019, **10**, 8840–8849; (*k*) J. Z. Du, C. Alvarez-Lamsfus, E. P. Wildman, A. J. Wooles, L. Maron and S. T. Liddle, *Nat. Commun.*, 2019, **10**, 4203; (*l*) J. Z. Du, D. M. King, L. Chatelain, E. L. Lu, F. Tuna, E. J. L. McInnes, A. J. Wooles, L. Maron and S. T. Liddle, *Chem. Sci.*, 2019, **10**, 3738–3745.

11 R. K. Thomson, T. Cantat, B. L. Scott, D. E. Morris, E. R. Batista and J. L. Kiplinger, *Nat. Chem.*, 2010, **2**, 723–729.
12 D. M. King, F. Tuna, E. J. L. McInnes, J. McMaster, W. Lewis, A. J. Blake and S. T. Liddle, *Science*, 2012, **337**, 717–720.
13 D. M. King, F. Tuna, E. J. L. McInnes, J. McMaster, W. Lewis, A. J. Blake and S. T. Liddle, *Nat. Chem.*, 2013, **5**, 482–488.
14 N. Tsoureas, A. F. R. Kilpatrick, C. J. Inman and F. G. N. Cloke, *Chem. Sci.*, 2016, **7**, 4624–4632.
15 P. A. Cleaves, D. M. King, C. E. Kefalidis, L. Maron, F. Tuna, E. J. L. McInnes, J. McMaster, W. Lewis, A. J. Blake and S. T. Liddle, *Angew. Chem., Int. Ed.*, 2014, **53**, 10412–10415.
16 K. C. Mullane, H. Ryu, T. Cheisson, L. N. Grant, J. Y. Park, B. C. Manor, P. J. Carroll, M.-H. Baik, D. J. Mindiola and E. J. Schelter, *J. Am. Chem. Soc.*, 2018, **140**, 11335–11340.
17 S. Fortier, J. R. Aguilar-Calderon, B. Vlaisavljevich, A. J. Metta-Magana, A. G. Goos and C. E. Botez, *Organometallics*, 2017, **36**, 4591–4599.
18 P. L. Diaconescu and C. C. Cummins, *Inorg. Chem.*, 2012, **51**, 2902–2916.
19 I. S. R. Karmel, N. Fridman, M. Tamm and M. S. Eisen, *J. Am. Chem. Soc.*, 2014, **136**, 17180–17192.
20 (*a*) S. Fortier, G. Wu and T. W. Hayton, *Dalton Trans.*, 2010, **39**, 352–354; (*b*) O. Bénaud, J.-C. Berthet, P. Thuéry and M. Ephritikhine, *Inorg. Chem.*, 2011, **50**, 12204–12214.
21 I. C. Tornieporthoetting and T. M. Klapotke, *Angew. Chem., Int. Ed.*, 1995, **34**, 511–520.
22 M. Castillo, A. J. Metta-Magana and S. Fortier, *New J. Chem.*, 2016, **40**, 1923–1926.
23 P. J. Fagan, J. M. Manriquez, S. H. Vollmer, C. S. Day, V. W. Day and T. J. Marks, *J. Am. Chem. Soc.*, 1981, **103**, 2206–2220.
24 I. Castro-Rodriguez, H. Nakai and K. Meyer, *Angew. Chem., Int. Ed.*, 2006, **45**, 2389–2392.
25 R. E. Cramer, F. Edelmann, A. L. Mori, S. Roth, J. W. Gilje, K. Tatsumi and A. Nakamura, *Organometallics*, 1988, **7**, 841–849.
26 A. R. Fox, P. L. Arnold and C. C. Cummins, *J. Am. Chem. Soc.*, 2010, **132**, 3250–3251.
27 J. J. Scepaniak, C. G. Margarit, J. N. Harvey and J. M. Smith, *Inorg. Chem.*, 2011, **50**, 9508–9517.
28 A. K. Maity, J. Murillo, A. J. Metta-Magana, B. Pinter and S. Fortier, *J. Am. Chem. Soc.*, 2017, **139**, 15691–15700.